

# Carbon Dioxide Activation and Reaction Induced by Electron Transfer at an Oxide–Metal Interface\*\*

Florencia Calaza,\* Christian Stiehler, Yuichi Fujimori, Martin Sterrer, Sebastian Beeg, Miguel Ruiz-Oses, Niklas Nilius, Markus Heyde, Teemu Parviainen, Karoliina Honkala, Hannu Häkkinen, and Hans-Joachim Freund

**Abstract:** A model system has been created to shuttle electrons through a metal–insulator–metal (MIM) structure to induce the formation of a CO<sub>2</sub> anion radical from adsorbed gas-phase carbon dioxide that subsequently reacts to form an oxalate species. The process is completely reversible, and thus allows the elementary steps involved to be studied at the atomic level. The oxalate species at the MIM interface have been identified locally by scanning tunneling microscopy, chemically by IR spectroscopy, and their formation verified by density functional calculations.

CO<sub>2</sub> is known to be one of the crucial greenhouse gases.<sup>[1]</sup> For decades, there have been efforts to store and utilize CO<sub>2</sub> in chemical reactions to transform a stable molecule into a useful chemical.<sup>[2]</sup> The crucial aspect is the transfer of an electron to the molecule,<sup>[3]</sup> which costs about 0.6 eV and is associated with a bending of the linear neutral CO<sub>2</sub> molecule.<sup>[4]</sup> This process may be understood on the basis of the so-called Walsh diagram<sup>[5]</sup> and it has been extensively discussed.<sup>[6]</sup> The free CO<sub>2</sub> radical anion is metastable with

respect to electron detachment and has a lifetime of a few milliseconds.<sup>[4b,d,7]</sup> By attaching a neutral CO<sub>2</sub> molecule to the radical anion, forming a (CO<sub>2</sub>)<sub>2</sub><sup>−</sup> species, a thermodynamically stable entity is formed in the gas-phase of a molecular beam experiment.<sup>[8]</sup> By transferring a second electron, the dimer anion may be transformed into an oxalate species whereby a carbon–carbon bond is formed. This compound may then be further transformed with water or ammonia to useful chemicals. It is therefore the key issue to transfer electrons. If one looks for a catalytic transformation to drive such a reaction, a source of electrons is needed that shuttles electrons back and forth between the reacting species. The goal herein is to describe and characterize a system that fulfills these requirements.

The concept presented herein is based on a metal–insulator–metal (MIM) system consisting of Au islands as an electron-storage material supported on a substrate that provides electrons to be shuttled back and forth between Au islands and adsorbed CO<sub>2</sub> (for conceptual overviews, see Ref. [9]). Specifically, the Au islands are located on an ultrathin MgO film, which covers a metallic substrate. Theoretical and experimental evidence has been provided of the negative charge of such Au islands, which assume a specific flat, raft-like morphology.<sup>[10,11]</sup> We have demonstrated that molecules such as CO,<sup>[12]</sup> and isophorone,<sup>[13]</sup> reside on the rim of such islands where the charge is localized for it to minimize electron–electron repulsion.<sup>[14]</sup> We will show in this study that the Au islands transfer electrons to carbon dioxide leading to the formation of a CO<sub>2</sub><sup>−</sup> radical ion, which may further react to form the oxalate. This model system may provide a playground to build upon a real catalytic system.

Figure 1 shows STM images of two Au islands on a bilayer MgO(001)/Ag(001) film. All experimental details explaining the deposition of the Au particles on ultrathin MgO are described in the Supporting Information. The morphology of the islands is, as proven before, two-dimensional with monolayer (ML) thickness.<sup>[11,15]</sup> Figure 1a shows a pristine cluster, which holds an average of 0.2 electrons per interface atoms that originate from the underlying metal substrate.<sup>[14]</sup> The additional electrons localize preferentially at the cluster edge and thus maximize the local density of the states at the rim (Figure 1c) resulting in the cluster edge to be the primary site for chemical reactions. This assumption is readily confirmed upon exposing the gold islands to CO<sub>2</sub> (Figure 1b,c). Molecular adsorbates become visible only at scanning values between −0.5 and +0.5 V. The CO<sub>2</sub> derivatives are exclusively adsorbed at the rim of the Au islands (Figure 1b), and

[\*] Dr. F. Calaza, C. Stiehler, Y. Fujimori, Prof. Dr. M. Sterrer,<sup>[†]</sup> S. Beeg, Dr. M. Ruiz-Oses, Prof. Dr. N. Nilius,<sup>[††]</sup> Dr. M. Heyde, Prof. Dr. H.-J. Freund

Department of Chemical Physics  
Fritz-Haber-Institut der Max-Planck-Gesellschaft  
Faradayweg 4-6, 14195 Berlin (Germany)  
E-mail: calaza@fhi-berlin.mpg.de

T. Parviainen, Prof. Dr. H. Häkkinen  
Department of Physics, Nanoscience Center  
University of Jyväskylä, 40014 Jyväskylä (Finland)  
Dr. K. Honkala, Prof. Dr. H. Häkkinen  
Department of Chemistry, Nanoscience Center  
University of Jyväskylä, 40014 Jyväskylä (Finland)

[†] Permanent address:  
Institute of Physics, University of Graz  
8010 Graz (Austria)

[††] Permanent address:  
Institute of Physics, Carl von Ossietzky Universität Oldenburg  
26111 Oldenburg (Germany)

[\*\*] We thank the Fonds der Chemischen Industrie as well as the Cluster of Excellence UNICAT, administered by the TU Berlin and funded through the German Science foundation, for financial support. F.C. is grateful to the Alexander-von-Humboldt foundation for a Georg Forster fellowship. C.S. thanks the Studienstiftung des Deutschen Volkes and Y.F. thanks DAAD and Co. Ltd. Takata for financial support. T.P. acknowledges Wihuri foundation for a personal PhD grant. We thank W.-D. Schneider for fruitful discussions.

Supporting information for this article is available on the WWW under <http://dx.doi.org/10.1002/anie.201501420>.

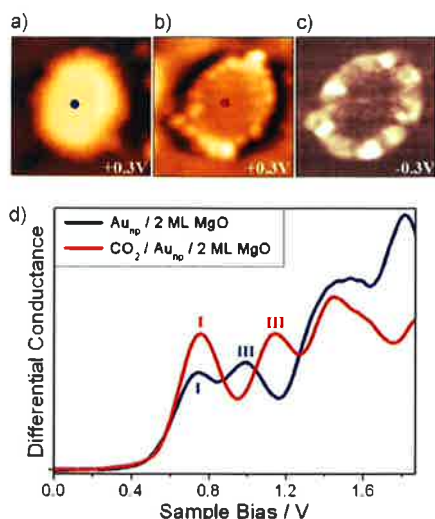


**Figure 1.** STM topographic images of a) a pristine Au cluster and b) after exposure to  $\text{CO}_2$  ( $8 \times 8 \text{ nm}^2$ , 50 pA). The Au clusters were prepared by evaporating Au on MgO mono- or bilayer films at 300 K and later exposed to 10–15 L  $\text{CO}_2$  at a temperature range 220 to 250 K. Molecules at the cluster perimeter in (b) become visible only when scanning at bias voltages between  $-0.5$  and  $0.5$  V. c) Corresponding  $dI/dV$  maps, displaying the high localization of electronic density at the negatively charged cluster edge. d)  $dI/dV$  spectra taken at the center of clusters shown in (a) (blue) and (b) (red). The positions of the first (I) and third (III) quantum well state in both spectra are indicated. Note the energy stretch of the internal energy scale of the cluster that is compatible with a  $\text{CO}_2$  induced decrease of the electron potential well formed by the Au island.

only to a small extent at specific sites at MgO films, as shown below. We count about 15 molecules for Au islands with an average size of  $5 \times 5 \text{ nm}^2$ . While for other molecules, such as isophorone, it has been possible to remove them via STM manipulation techniques,  $\text{CO}_2$  and its reaction products are strongly bound to the Au islands and cannot be displaced. The consequences on the electronic structure of the clusters were investigated by  $dI/dV$  spectroscopy and mapping.<sup>[13]</sup> The quantum well states (QWS), which develop in the electronic structure of the 2D gold islands,<sup>[15,16]</sup> experience a characteristic shift after molecular adsorption (Figure 1 d). In fact, the internal energy scale of the cluster seems stretched, that is, the energy shift of the upper QWS is larger than of the lower ones. Apparently,  $\text{CO}_2$  adsorption reduces the dimension of the gold-related quantum well, for instance by suppressing the spill-out of gold wave function as a result of repulsive interactions with the adsorbates.

Figure 2a (top) shows an IR spectrum of a clean MgO ultrathin film that has been exposed to  $\text{CO}_2$  at 220 K, close to saturation coverage. There is one band observed at  $1295 \text{ cm}^{-1}$ . The intensity of this band corresponds to 0.02 ML of molecules as determined by calibration measurements on the  $\text{CO}/\text{Pd}(111)$  system and coverage-dependent LEED data. This coverage is consistent with the number of color ( $\text{F}^+$ ) centers on the surface, located specifically at MgO edge sites as independently determined through STS measurements.<sup>[17]</sup> The observed frequency would be compatible with both

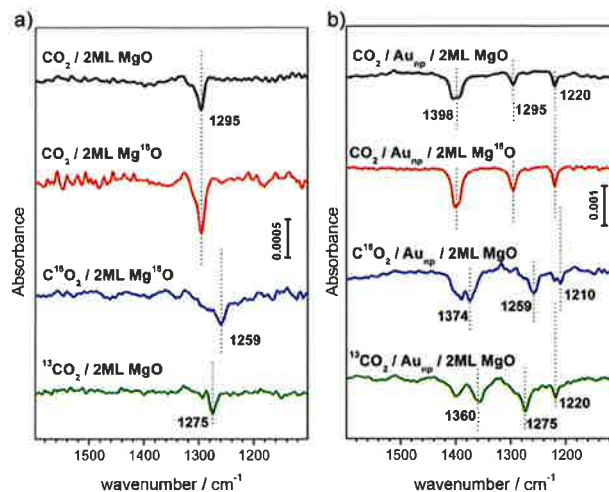


**Figure 2.** a)  $\text{CO}_2$  adsorption (saturation dose at 220 K) on 2 ML MgO-(001)/Ag(001). b)  $\text{CO}_2$  adsorption (saturation dose at 220 K) on Au clusters (Au coverage approximately 0.06 ML) deposited on 2 ML MgO(001)/Ag(001).

carbonate, that is,  $\text{CO}_2$  adsorbed on top of lattice oxygen, as well as with the formation of a carboxylate, where the molecule would reside on an oxygen vacancy or on a metal ion.<sup>[18]</sup> The carbonate formation may be ruled out by measuring IR spectra after dosing  $\text{CO}_2$  on MgO films prepared with isotope-labeled oxygen ( $^{18}\text{O}_2$ ). The observed band does not shift to lower frequency, as would be expected for carbonate formation, because one of the masses of the carbonate would be an  $^{18}\text{O}$  atom. If, on the other hand, the  $\text{CO}_2$  is either oxygen- or carbon-labeled, the frequency of the carboxylate shifts as expected to  $1259 \text{ cm}^{-1}$  and to  $1275 \text{ cm}^{-1}$ , respectively (Figure 2 a). The frequency as well as an adsorption site possibly on top of a  $\text{F}^+$  center is also consistent with calculations from various groups for  $\text{CO}_2$  adsorption on bulk MgO(100) surfaces.<sup>[19]</sup> A full study of  $\text{CO}_2$  adsorption on a thin MgO(100) film supported on Ag(001) has not been published to date. The results reported for a bulk MgO(001) may not be directly applicable here owing to the absence of the metal support.

If  $\text{CO}_2$  is dosed onto Au islands supported on MgO, new vibrational bands are observed. The coverage of Au was 0.06 ML. The IR spectra of this system at  $\text{CO}_2$  saturation exposure are shown in Figure 2b (top). Three bands are observed; the band at  $1294 \text{ cm}^{-1}$  has been identified above and may be used as a calibration standard. The other two bands centered at  $1220 \text{ cm}^{-1}$  and  $1398 \text{ cm}^{-1}$  are assigned to oxalate. There is certain degree of heterogeneity in those bands owing to the irregular rim shape of the Au islands. The amount of adsorbed molecules as calculated from the region of the MgO surface covered by Au islands of 4–5 nm diameter (average nanoparticle size; Supporting Information, Figure S1) agrees well with the observed intensities assuming 15 molecules per island adsorbed. The basis for assigning the molecules to oxalate species comes from a comparison with known oxalate transition metal complexes,<sup>[20]</sup> which exhibit two bands with appropriate vibrational frequencies.

Further evidence is again derived from isotopic labeling experiments. First, when labeling the oxide film ( $\text{Mg}^{18}\text{O}$ ), we observed no shifts of any of the bands, thus ruling out the possibility that oxygen atoms at the cluster rim are responsible for anchoring the  $\text{CO}_2$ . As evident from Figure 2b, the band shift upon  $\text{CO}_2$  labeling is consistent with the assignment based on metal oxalate complexes. There are also unavoidable bands that are due to unlabeled  $\text{CO}_2$  from the background. In particular, for  $^{18}\text{O}$ -labeled  $\text{CO}_2$ , the carboxylate at MgO sites shifts to  $1258\text{ cm}^{-1}$  as before, and the other two bands shift to  $1374\text{ cm}^{-1}$  and  $1210\text{ cm}^{-1}$ , respectively. Upon  $^{13}\text{C}$ -labeling, the carboxylate shifts to  $1274\text{ cm}^{-1}$  while the band at  $1220\text{ cm}^{-1}$  does not shift, and the higher-frequency band moves to  $1360\text{ cm}^{-1}$ . For the two oxalate modes, a normal mode analysis is available, performed for a planar oxalate arrangement, and the in-plane vibrational frequencies have been calculated.<sup>[20]</sup> Those calculations reveal that the  $1220\text{ cm}^{-1}$  band has predominantly C–O stretch and O–C–O angle deformation character, while the  $1398\text{ cm}^{-1}$  band has predominantly C–C stretch character with some C–O stretch contributions mixed in. The observed isotopic shifts are fully consistent with those qualitative assignments and support strongly the assignment of the two observed peaks to oxalate species formed at the rim of the Au islands.

Several representative adsorption configurations of  $\text{CO}_2$  and  $\text{C}_2\text{O}_4$  species at an Au ad-atom and an  $\text{Au}_2$  ad-dimer attached to a  $\text{MgO}(001)/\text{Ag}(001)$  film were investigated by DFT calculations (Figure 3; Table S1). Two configurations for an  $\text{AuCO}_2$  ad-complex were found, which are a surface-planar and surface-normal  $\text{CO}_2$  species bound at the side of the Au atom (Figure 3a,b). In the surface-planar configuration, the Au ad-atom transfers  $-0.7|e|$  to  $\text{CO}_2$ , resulting in an adsorption energy of  $-0.58\text{ eV}$ . In the surface-normal configuration, the charge transfer is slightly larger but the adsorp-

tion is weaker than in the case of the clean film. Similar two configurations are found for  $\text{CO}_2$  adsorption on the  $\text{Au}_2$  ad-dimer. There, both the  $\text{CO}_2$  binding energy and the amount of charge transfer are clearly increased suggesting an even stronger  $\text{CO}_2$  binding for larger Au ad-clusters (Table S1).

We turn next to calculations on the oxalate  $\text{C}_2\text{O}_4^{2-}$  species. We found two gas-phase configurations (“cross” and planar) with C–C bond lengths of  $1.61$  and  $1.70\text{ \AA}$ , respectively (Figure 3c,d). These species were converged to a stable minimum with a total charge of  $-1.8|e|$  in the complex, approximating closely the full double anion. When this complex is bound to the  $\text{Au}_2$  ad-cluster, again two configurations were found, with adsorption energies of  $-0.95\text{ eV}$  for the “C–C surface-planar” and  $-0.72\text{ eV}$  for the “C–C surface-normal” (Figure 3e,f and 3g,h). The C–C bond length is reduced here to  $1.56\text{ \AA}$  and  $1.53\text{ \AA}$ , respectively, and the charge on the  $\text{C}_2\text{O}_4$  part is  $-1.59|e|$  and  $-1.55|e|$  (Table S1) with the gold atom next to the complex being clearly positively charged (Figure 3e,g). Our calculations suggest that the formation of the oxalate is an activated process, as the formation of the stable gold–oxalate complex seems to depend sensitively on the reaction coordinate.

Vibrational analysis was performed at the  $\text{Au}_2$ -oxalate species as well (Table S1). We note that the “C–C surface-normal” configuration (Figure 3h,i) has eigenmodes at  $1228\text{ cm}^{-1}$  and  $1414\text{ cm}^{-1}$ , which are not far from the observed frequencies at  $1220\text{ cm}^{-1}$  and  $1398\text{ cm}^{-1}$  in Figure 2b.

We have also performed temperature-programmed desorption experiments to identify desorbing species. Only  $\text{CO}_2$  is detected desorbing from the surface and representative TPD spectra are shown in Figure S2. Two desorption states have been identified: The carboxylate species desorbs between  $280$  and  $310\text{ K}$ , while the oxalate species has desorbed at  $340\text{ K}$  according to Equation (1):

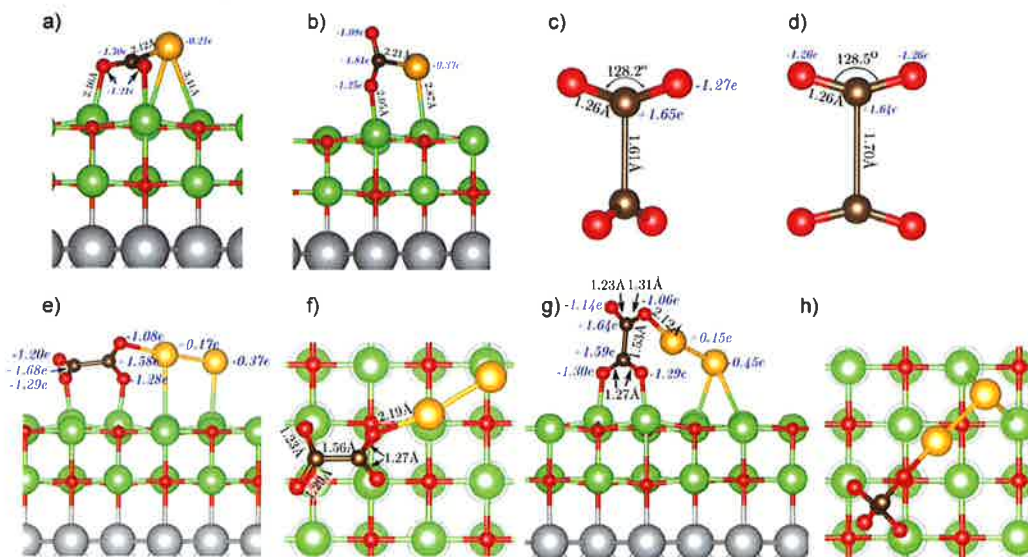
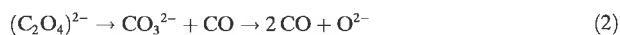


**Figure 3.** Computed structures of  $\text{CO}_2^-$  and  $\text{C}_2\text{O}_4^{2-}$  species. a,b) two configurations of  $\text{CO}_2^-$  bound at a single Au ad-atom; c,d) “cross” and planar structures of gas-phase  $\text{C}_2\text{O}_4^{2-}$ ; e,f) side and top views of a “cross”  $\text{C}_2\text{O}_4^{2-}$  bound at the gold ad-dimer having a surface-planar C–C bond; g,h) side and top views of the “cross”  $\text{C}_2\text{O}_4^{2-}$  bound at the gold ad-dimer having a surface-normal C–C bond. Colors: Mg green, O red, C brown, Au yellow, Ag gray. The blue italics denote atomic Bader charges and black roman numerals interatomic bond lengths and bond angles. The gas-phase structures in (c) and (d) were converged for the total charge of  $-1.8|e|$  (see text).



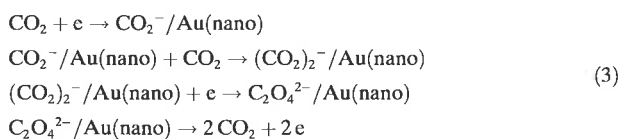


This is by no means self-evident, as in former studies on adsorbed oxalates, an alternate route of decomposition has been observed, as given in Equation (2):<sup>[21]</sup>



In this scenario, also CO desorption should be observable and oxygen would remain on the surface limiting the reversibility of the process. In the present case, CO<sub>2</sub> adsorption–desorption experiments reveal that the process is entirely reversible. One reason for the reversible oxalate–carbon dioxide adsorption–desorption is the low oxophilicity of Au, which hampers the formation of adsorbed carbonate and thus the alternate reaction route. This reversibility renders our system a well-suited model system to study electron shuttling-induced reactions at surfaces.

Our experimental and computational results presented above strongly suggest the following scenario at the supported Au islands on a ultrathin MgO(001) film: The ultrathin MgO(001) film grown on a Ag(001) surface shuttles electrons to nanoscopic Au islands, which assume a flat, raft-like morphology with the transferred electrons located at the rim of the raft. Carbon dioxide adsorbs at the rim of the nano islands, transforms into carboxylate by electron transfer, which then reacts with another CO<sub>2</sub> molecule to form oxalate according to Equation (3):



The formed oxalate desorbs from the surface as carbon dioxide and the electrons are shuttled back to the Au islands. The reaction is fully reversible. Evidence for the oxalate C<sub>2</sub>O<sub>4</sub><sup>2-</sup> intermediate is found from the IRAS data and supported by DFT calculations on oxalate adsorption on supported Au<sub>2</sub> cluster on the MgO film. Further experimental and computational investigations will be conducted to fully characterize the intermediates and to reveal activation barriers of the above-mentioned reaction at the gold island edges.

**Keywords:** carbon dioxide · electron transfer · metal–insulator–metal structure · oxalate · oxygen

[1] United Nations Framework Convention on Climate Change, at [http://unfccc.int/ghg\\_data/items/3800.php](http://unfccc.int/ghg_data/items/3800.php).

[2] a) *Carbon Dioxide as Chemical Feedstock* (Ed.: M. Aresta), Wiley-VCH, Weinheim, 2010; b) K. Weissermel, H.-J. Arpe, *Industrielle organische Chemie*, Verlag Chemie, Weinheim, 1978; c) J. Paul, C.-M. Pradier, *Carbon Dioxide Chemistry: Environmental Issues, Special Publication No. 153*, The Royal Society of Chemistry, London, 1994; d) *Methane Conversion, Proceedings of a Symposium on the Production of Fuels and Chemicals from*

- Natural Gas. Vol. 36* (Eds.: D. M. Bibby, C. D. Chang, R. F. Howe, S. Yurchak), Elsevier, Amsterdam, 1988; e) S. Teuner, *Hydrocarbon Process.* 1985, 64, 106; f) F. Solymosi, G. Kutsán, A. Erdöhelyi, *Catal. Lett.* 1991, 11, 149; g) M. M. Halmann, M. Steinberg, *Greenhouse Gas Carbon Dioxide Mitigation: Science and Technology*, CRC, Boca Raton, 1998; h) E. E. Benson, C. P. Kubiak, A. J. Sathrum, J. M. Smicja, *Chem. Soc. Rev.* 2009, 38, 89; i) W. Wang, S. Wang, X. Ma, J. Gong, *Chem. Soc. Rev.* 2011, 40, 3703; j) D. Preti, C. Resta, S. Squarzialupi, G. Fachinetti, *Angew. Chem. Int. Ed.* 2011, 50, 12551; *Angew. Chem.* 2011, 123, 12759; k) W. Zhu, R. Michalsky, Ö. Metin, H. Lv, S. Guo, C. J. Wright, X. Sun, A. A. Peterson, S. Sun, *J. Am. Chem. Soc.* 2013, 135, 16833.
- [3] a) H.-J. Freund, M. W. Roberts, *Surf. Sci. Rep.* 1996, 25, 225; b) F. Solymosi, *J. Mol. Catal.* 1991, 65, 337.
- [4] a) K. O. Hartman, I. C. Hisatsune, *J. Chem. Phys.* 1966, 44, 1913; b) R. N. Compton, P. W. Reinhardt, C. D. Cooper, *J. Chem. Phys.* 1975, 63, 3821; c) J. Pacansky, U. Wahlgren, P. S. Bagus, *J. Chem. Phys.* 1975, 62, 2740; d) D. Schröder, C. A. Schalley, J. N. Harvey, H. Schwarz, *Int. J. Mass Spectrom.* 1999, 185–187, 25.
- [5] A. D. Walsh, *J. Chem. Soc.* 1953, 2260.
- [6] T. Sommerfeld, H.-D. Meyer, L. S. Cederbaum, *Phys. Chem. Chem. Phys.* 2004, 6, 42.
- [7] U. Burghaus, *Prog. Surf. Sci.* 2014, 89, 161.
- [8] a) A. Stamatovic, K. Stephan, T. D. Märk, *Int. J. Mass Spectrom. Ion Processes* 1985, 63, 37; b) M. Knapp, O. Echt, D. Kreisler, T. D. Märk, E. Rocknagel, *Chem. Phys. Lett.* 1986, 126, 225; c) E. L. Quitevis, D. R. Herschbach, *J. Phys. Chem.* 1989, 93, 1136; d) M. Lezius, T. Rauth, V. Grill, M. Foltin, T. D. Märk, *Z. Phys. D* 1992, 24, 289.
- [9] a) H. J. Freund, N. Nilius, T. Risse, S. Schauermaun, *Phys. Chem. Chem. Phys.* 2014, 16, 8148; b) T. Risse, S. Shaikhutdinov, N. Nilius, M. Sterrer, H.-J. Freund, *Acc. Chem. Res.* 2008, 41, 949.
- [10] D. Ricci, A. Bongiorno, G. Pacchioni, U. Landman, *Phys. Rev. Lett.* 2006, 97, 036106.
- [11] M. Sterrer, T. Risse, M. Heyde, H.-P. Rust, H.-J. Freund, *Phys. Rev. Lett.* 2007, 98, 206103.
- [12] X. Lin, B. Yang, H. M. Benia, P. Myrach, M. Yulikov, A. Aumer, M. Brown, M. Sterrer, O. Bondarchuk, E. Kieseritzky, J. Rucker, T. Risse, H. Gao, N. Nilius, H. J. Freund, *J. Am. Chem. Soc.* 2010, 132, 7745.
- [13] C. Stiehler, F. Calaza, W.-D. Schneider, N. Nilius, H.-J. Freund, submitted.
- [14] X. Lin, N. Nilius, M. Sterrer, P. Koskinen, H. Häkkinen, H.-J. Freund, *Phys. Rev. B* 2010, 81, 153406.
- [15] X. Lin, N. Nilius, H. J. Freund, M. Walter, P. Frondelius, K. Honkala, H. Häkkinen, *Phys. Rev. Lett.* 2009, 102, 206801.
- [16] C. Stiehler, Y. Pan, W.-D. Schneider, P. Koskinen, H. Häkkinen, N. Nilius, H.-J. Freund, *Phys. Rev. B* 2013, 88, 115415.
- [17] M. Sterrer, M. Nowicki, M. Heyde, N. Nilius, T. Risse, H.-P. Rust, G. Pacchioni, H.-J. Freund, *J. Phys. Chem. B* 2006, 110, 46.
- [18] O. Seiferth, K. Wolter, B. Dillmann, G. Klivenyi, H. J. Freund, D. Scarano, A. Zecchina, *Surf. Sci.* 1999, 421, 176.
- [19] a) G. Pacchioni, *ChemPhysChem* 2003, 4, 1041; b) G. Preda, G. Pacchioni, M. Chiesa, E. Giamello, *J. Phys. Chem. C* 2008, 112, 19568; c) C. A. Downing, A. A. Sokol, C. R. A. Catlow, *Phys. Chem. Chem. Phys.* 2014, 16, 184.
- [20] J. Fujita, A. E. Martell, K. Nakamoto, *J. Chem. Phys.* 1962, 36, 339.
- [21] a) J. Paul, F. M. Hoffmann, L. L. Robbins, *J. Phys. Chem.* 1988, 92, 6967; b) F. M. Hoffmann, M. D. Weisel, J. Paul, *Surf. Sci.* 1994, 316, 277; c) R. L. Toomes, D. A. King, *Surf. Sci.* 1996, 349, 65.

Received: February 12, 2015

Revised: March 15, 2015

Published online: May 26, 2015